A Novel UWB Vivaldi Antenna Array for Radar Applications

Osama M. Dardeer, Tamer G. Abouelnaga, Ashraf S. Mohra, Hadia M. El-Hennawy

Abstract— This paper presents a novel four elements ultra wideband (UWB) antipodal Vivaldi antenna (AVA) array design for radar and microwave imaging applications. Initially, the radiation ares of the AVA is designed based on an elliptical curve shape. Next, the substrate end is shaped as a triangular shape and a negative index metamaterial (NIM) has been incorporated into the AVA aperture to act as a director. A gain enhancement of 2 dB is obtained for the proposed element compared to conventional one. The proposed antenna element is fabricated and measured. There is a good consistency between the simulated and measured return loss. In addition, four UWB Vivaldi antennas with substrate end shaping are placed along the z-axis in a linear antenna array configuration. The four NIM structures of the four antennas are placed together to form a sheet which is perpendicular to the four antenna substrates. A gain enhancement of about 6 dBi is obtained compared to the proposed single element through the whole UWB frequency range. The proposed antenna array bandwidth extends from 3 GHz to 16 GHz. The proposed antenna array is fabricated, measured, and good agreement is obtained between simulated and measured reflection coeffcients.

Index Terms— Ultra-Wideband, Vivaldi Antenna, Linear Antenna Array, Radar Applications.

1 Introduction

THE Federal Communication Committee (FCC) has approved the frequency band between 3.1 to 10.6 GHz for ultra wideband (UWB) applications in 2002 [1]. There are great attentions from the academic and industrial communities to this UWB radio system which is 7.5 GHz wide. Designing a UWB antenna with stable endfire radiation patterns and high gain remains a challenge still. This kind of antennas finds lots of applications like radar, remote sensing, microwave imaging, and UWB communication systems. Planar antennas are preferred because of the merits of lightweight, low profile, and cost effective [2]. Tapered slot antenna (TSA) is a good candidate to achieve wide impedance bandwidth, stable radiation pattern, and high gain characteristics [3]. However, the antipodal Vivaldi antenna (AVA) provides more compact size and lower reflections from the feeding structure than TSA [4]. It is worthy to note that balanced antipodal Vivaldi antenna (BAVA) is a compact and versatile design that was introduced by Langley et al. [5]. The unique characteristics of the Vivaldi antenna enabled it to be used in many applications where UWB and end fire radiation pattern is required like high range radar systems [6], detection of on-body concealed weapons [7], see through wall applications [8], and imaging of tissues for the detection of cancerous cells [9]. For these applications, the antenna should achieve wide impedance bandwidth, narrow half power beamwidth, and high gain. Different antennas in [10], [11], [12], [13], [14], [15], [16], [17], [18] are presented to fulfill these requirements.

In this paper, the shape of the radiation flares is designed in the form of elliptical curves. The basic design has been explained analytically and the equations governing the elliptical curves has been presented. Next, a negative index metamaterial (NIM) has been incorporated into the AVA aperture to act as a director. The proposed element signicantly improves the antenna radiation pattern and gain. In addition, this element is used in a four element UWB antenna array that operates from 3—16 GHz with more than 12 dBi maximum gain. The paper is organized as follows. Section 2 describes the configuration of the proposed antenna element. Section 3 is devoted to the 4-element array. The paper is concluded in Section 4.

2 Proposed Antenna Element

2.1 Antipodal Vivaldi Antenna Design

The antenna is designed on a low cost FR4 substrate with dielectric constant ε_r=4.3, thickness h=1.5 mm, and loss tangent δ=0.025. The antenna geometry is shown in Fig. 1. The proposed antenna includes three parts: microstrip line feed section, transition section and radiating section. Transition section is the most critical part in the antenna design since it is a gradient structure and acts as a balun. This section is formed by intersecting two identical half ellipses with the top and bottom metals besides an offset distance from the beginning of the feed line. The shape of the radiation are is designed in the form of elliptical curve. This taper line is a quarter elliptical arc of different major/ minor axis ratio to form a smooth transition to reduce reflection. As a consequence, this elliptical configuration provides a good broadband characteristics and it is one of the optimum curvatures [19].

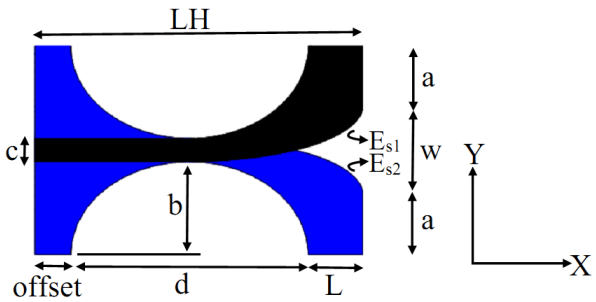

Figure 1: Antipodal Vivaldi antenna geometry.

Theoretically, Vivaldi antenna has infinite bandwidth [20] and

generally the bandwidth of the Vivaldi antenna is proportional to its length and aperture. Therefore, the size of the antenna increases when UWB performance is required. The lower frequency limit depends on the length of antenna and the effective dielectric constant ε_{eff}. Lower frequency limit is calculated from [21]:

$$f_{\min} = [c/2(LH)(\sqrt{\varepsilon_{eff}})] \quad (1)$$

$$\varepsilon_{eff} = [(\varepsilon_r + 1)/2] + [(\varepsilon_r - 1)/2][1 + (12h/LH)]^{-0.5} \quad (2)$$

where h is the substrate height and LH is the antenna length. The structural parameters are listed in Table 1, and have already been optimized. Extensive parametric studies are carried out using Computer Simulation Technology Microwave Studio (CST MWS) to study the effect of different parameters on the antenna performance to select the proper dimensions of the major and minor axes of the intersecting ellipses. The dimensions of the antenna are 60 × 45 × 1.5 mm^3. As shown in Fig. 1, the shape of the radiation flare is designed in the form of elliptical curve. This taper line is a quarter elliptical arc and the two curves are denoted: Es1 and Es2. In the equations describing the two curves, u and v represent the major and minor axes respectively. Using the structural parameters in Table 1, the two elliptical curves can be described by the equations:

E_{s1}:

$$y = [-v\sqrt{1-[x-(offset+d/2)]^2/u^2}] + (2b+c-a)$$
$$, (offset + d/2 \le x \le LH) \quad (3)$$

E_{s2}:

$$y = [-v\sqrt{1-[x-(offset+d/2)]^2/u^2}] + (a)$$
$$, (offset + d/2 \le x \le LH) \quad (4)$$

TABLE 1: STRUCTURAL PARAMETERS OF THE PROPOSED AVA.

B	16 mm	LH	60 mm
C	4 mm	L	LH-offset-d
D	43.5097 mm	a	(2b+c-w)/2
offset	6.53 mm	u	LH-(offset+d/2)
W	15.0794 mm	v	b+c-a

Fig. 2a shows the effect of length d on the proposed antenna bandwidth performance. An enhancement of 8 dB is obtained as d changes from 48.5 mm to 43.5 mm at 6 GHz. Also, an enhancement of 2 dB is obtained at 10 GHz. As a result, d is chosen to be 43.5 mm. The offset length is chosen to be 6.53 mm in order to achieve wide impedance bandwidth with good return loss as shown in Fig. 2b. When the antenna aperture width w gets smaller, the antenna has a better return loss in low frequency, but from the point of view of the antenna gain, it gets worse as shown in Fig. 2c. Therefore, when the width w increases, the gain is enhanced and the resonance point is shifted to high frequency because the current path becomes shorter as illustrated in Fig. 3.

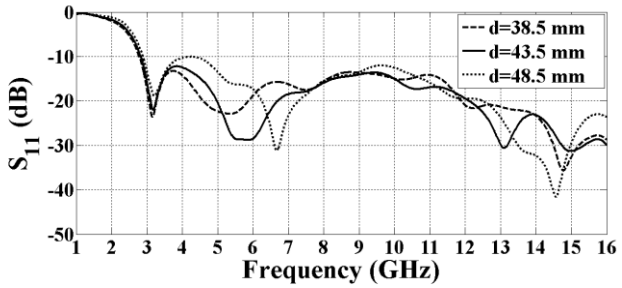

(a)

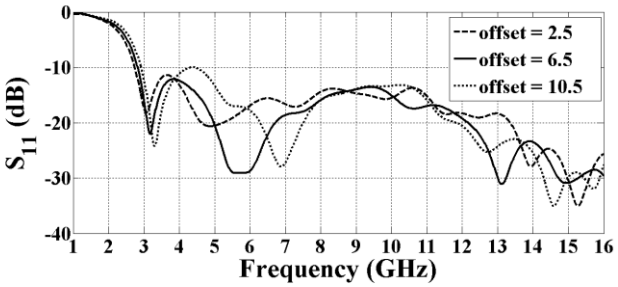

(b)

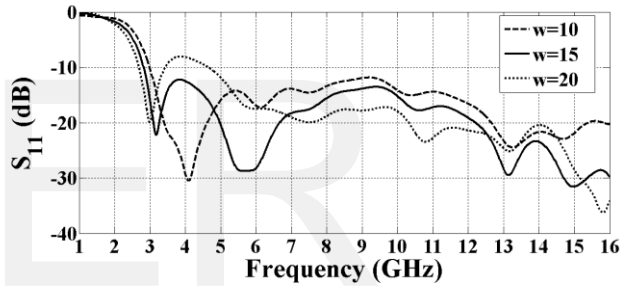

(c)

Fig. 2 (a) Simulated return loss of antenna with different d, (b) different offset at d = 43.5 mm. (c), different w at d = 43.5 mm and offset=6.5 mm.

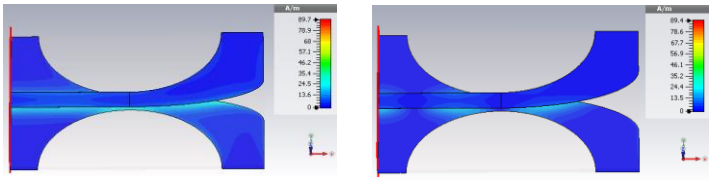

(a) (b)

Fig. 3 (a) Current distribution at w=10mm, (b) w =15mm.

2.2 Substrate End Shaping

Normally antipodal Vivaldi antennas suffer from low axial gains and tilted beams. The technique proposed in [18] has been applied here to correct both problems. This technique is based on the substrate end shaping. It is a simple geometrical medication that extends the substrate beyond its length to an appropriate length. This extended length acts as a lens and can be considered as an integral part of the antenna in order to be easy to fabricate. A triangular end shaping is considered since it produced the highest improvement in gain throughout the entire frequency band of operation. This triangle is equilateral and extends for a distance of half the antenna length which is 30 mm. There is an enhancement of 2 dB when substrate end shaping is applied, and this can be illustrated in Fig. 4.

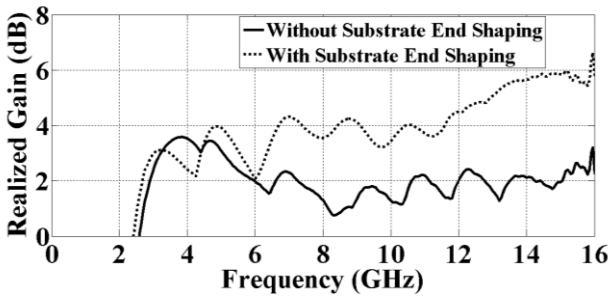

Fig. 4 Effect of the substrate end shaping on the realized gain.

2.3 Negative Index Metamaterial Structure

Metamaterial is a manmade composite structure made of dielectrics metals. It implies that it is not a homogenous material, rather inhomogeneous artificial. Metallic or dielectric structures in metamaterials are typically much smaller than the wavelength. So, at a wavelength scale, one can assume an effectively homogenous material but with very different physical properties. So, material could be divided as, first a positive ε and μ material, this kind of materials is called double positive materials or natural dielectric materials. If an electromagnetic wave propagates in such a material, you will see a propagating wave with some loss or attenuation. Second, a negative ε and a positive μ such as metals, thus metals are also called epsilon negative materials. If electromagnetic wave propagates in a metal, it experiences huge attenuation that is why when metals are discussed, the skin depth effect is discussed too. Actually the waves will attenuate a lot into the metamaterials.

In 1960s, materials having simultaneously negative μ and negative ε are theoretically proposed and they produce a negative refraction index. This materials are called a left handed material [22]. In 1996, negative epsilon material could be obtained by arranging the metal wires in a simple cubic lattice. But the problem still remained how a negative μ could be obtained. In 2000 by smith, the question was answered where a structure consisting of periodic array of split ring resonators and continuous wires that produced the negative permeability and negative permittivity is proposed [23], [24].

Fig. 5 shows a NIM structure unit cell. It is constructed of two self complementary archimedean rectangular spiral shapes. The NIM unit cell with dimensions of 10×10 mm^2 (A×B) is designed on an identical substrate material that is used for the AVA design. The NIM is excited with an electric field along the y-direction and a magnetic field along x-direction as illustrated in Fig. 6. The resonant frequency of NIM cell is controlled by the gap between spirals [14], [15]. The incorporation of NIM in addition to the substrate end shaping did not signicantly affect the return loss (S_{11}) of the antenna.

Different techniques are available for incorporating NIM into AVA. In this paper, single layer of NIM is inserted perpendicularly to the substrate i.e. between the two arms of the antenna. The final structure of the NIM incorporated AVA with substrate end shaping is shown in Fig. 7. A further increment of extended length beyond three NIM cells is not desirable for practical applications, in addition to the simplicity of fabrication.

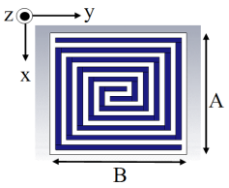

Fig. 5 NIM unit cell.

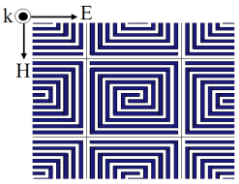

Fig. 6 NIM configuration.

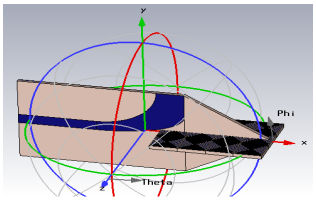

Fig. 7 The proposed NIM incorporated AVA with substrate end shaping.

2.4 Proposed Antenna Radiation Pattern

The simulated and measured radiation patterns of the antenna are shown in Figs. 8—10. From these figures, it is found that the proposed antenna exhibits good unidirectional radiation patterns in the elevation and azimuth planes. Over the operating frequency band, the main lobes of the radiation patterns are fixed in the end fire direction (x-axis direction).

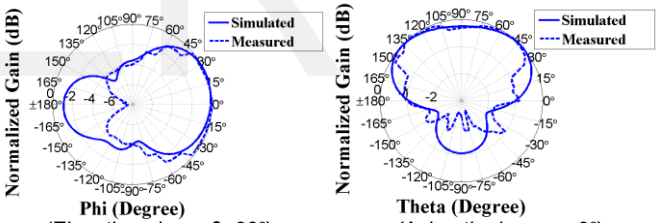

(Elevation plane, θ=90º) (Azimuth plane, φ=0º)

Fig. 8 Normalized radiation pattern of the antenna at 3.2 GHz.

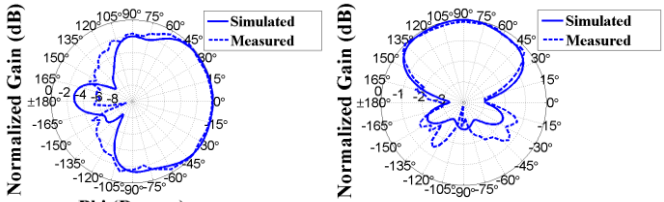

(Elevation plane, θ=90º) (Azimuth plane, φ=0º)

Fig. 9 Normalized radiation pattern of the antenna at 6 GHz.

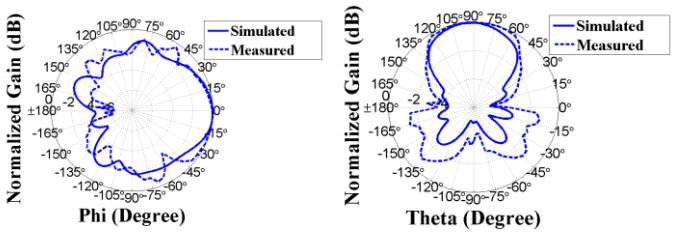

(Elevation plane, θ=90º) (Azimuth plane, φ=0º)

Fig. 10 Normalized radiation pattern of the antenna at 9.7 GHz.

2.5 Fabrication and Measurement of The Proposed Antenna Element

The bandwidth of the proposed antenna extends from 2.8 to 16 GHz. The fabricated antenna is shown in Fig. 11. Fig. 12 presents the simulated and measured return loss of proposed antenna. There is a good agreement between the two results. The difference between simulated and measured S_{11} may come from the connection loss between the printed circuit board and SMA connector, and the unstability of the FR4 substrate parameters at 12 GHz.

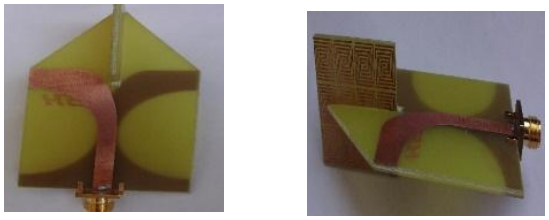

Fig. 11 Photograph of the fabricated antenna.

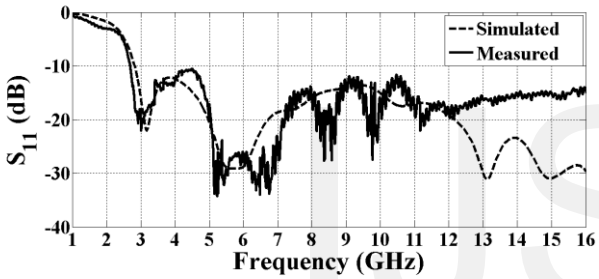

Fig. 12 Return loss performance of the proposed antenna.

3 PROPOSED 4-ELEMENT ARRAY

3.1 Array Configuration

In order to obtain better range resolution in a radar system, a wide bandwidth is required. Also, for two adjacent targets at the same range, they must be separated by at least one beamwidth to be distinguished as two objects. Bilgic and Yegin in [25] achieved 13.5° half power beamwidth but covers only the frequency band from 8.75 to 12.25 GHz. In this paper, four UWB Vivaldi antennas with substrate end shaping are placed along the z-axis in a linear array configuration as shown in Fig. 13. The Dolph-Tschebysche distribution with a side lobe level (SLL) of -20 dB has been chosen for this design. Accordingly, the four excitation coefficients are (0.576—1—1—0.576). The four NIM structures of the four antennas are assembled together to form a large sheet which is perpendicular to the four substrates. This structure is proposed due to high gain features.

For narrow band antenna arrays, the element spacing should be less than one wavelength (λ) to avoid the grating lobes. Moreover, it should be greater than half wavelength (λ/ 2) to minimize the fading correlation and mutual coupling between elements. This spacing is not obvious in ultra-wideband antenna arrays to avoid the grating lobes in the whole UWB frequency span since they operate at very large frequency bandwidth [26].

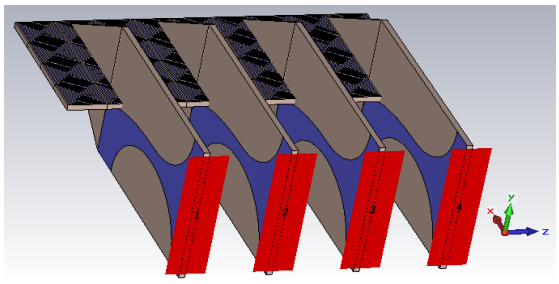

Fig. 13 Array Configuration.

3.2 Element Spacing

Many trials are carried out to choose properly the distance between elements which is the most important parameter that affects mutual coupling. Of course, a large distance results in less mutual coupling effects, and consequently a better isolation between array elements can be achieved, while the SLL will be deteriorated. There is always a trade-off between half power beamwidth (HPBW) and SLL [27]. Table 2 lists different values of the element spacing, HPBW and SLL in both the elevation and azimuth planes at 10 GHz.

TABLE 2 HPBW AND SLL FOR DIFFERENT ELEMENT SPACING AT 10 GHZ.

Element Spacing	Elevation plane (XY-plane)		Azimuth plane (XZ-plane)	
	HPBW	SLL	HPBW	SLL
22 mm	50.9°	-5.2 dB	19.1°	-20 dB
25 mm	54.1°	-4.1 dB	17°	-21.8 dB
30 mm	57.2°	-4 dB	14.1°	-20.3 dB

3.3 Realized Gain

Figure 14 shows the antenna gain for single element and array structures for the UWB frequency range. In the frequency bands between 3 GHz and 9 GHz, the array gain is about 5 dBi more than the single element gain and exceeds 6 dBi beyond 9 GHz. If the element spacing is increased from (λ/ 2) until (λ), the array gain is increased. This spacing shouldn't exceed one wavelength to avoid the grating lobes. The azimuth plane radiation pattern comparison between a single element and a 4-element antenna array is shown in Fig. 15.

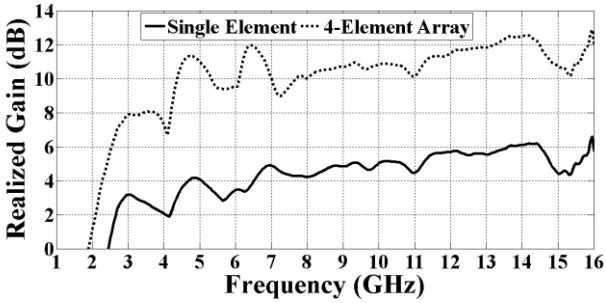

Fig. 14 Array and single element antenna gain at 25 mm element spacing.

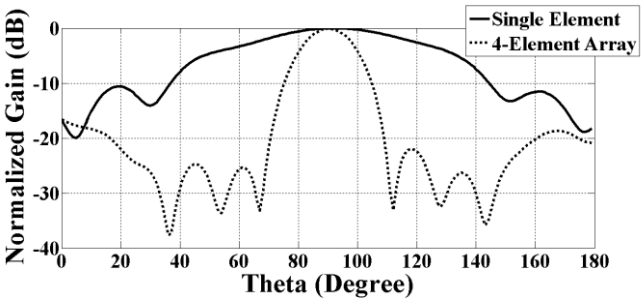

Fig. 15 Azimuth radiation pattern at 10 GHz and 25 mm element spacing.

3.4 Fabrication and Measurement of The Proposed Four Element Antenna Array

The fabricated four element antenna array is shown in Fig. 16. Fig. 17 presents the simulated and measured return loss (S_{11}) of proposed array. The two results are below -10 dB across the entire frequency band of operation.

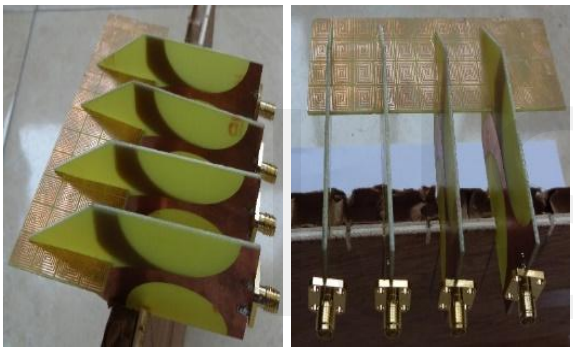

Fig. 16 Photograph of the fabricated antenna array.

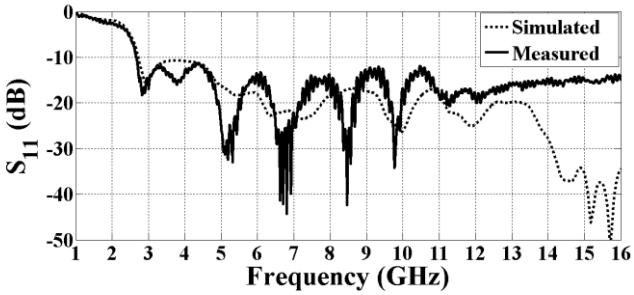

Fig. 17 Return loss of the antenna array.

4 Conclusion

This paper presents a UWB AVA with radiation flares in the form of elliptical curves. The antenna dimensions are 60 × 45 × 1.5 mm^3 with a triangular shape extension and a NIM perpendicular to the substrate. The proposed element is capable of achieving an input impedance bandwidth from 2.8 GHz to 16 GHz experimentally. Then, four identical antenna elements were employed to introduce a linear array. The excitation coefficients were calculated according to the Dolph-Tschebysche distribution. A prototype of the proposed single and four elements antenna array were fabricated and measured over the UWB frequency range. Good agreement was obtained between measured and simulated reflection coefficients. The antenna array gain was increased by about 6 dBi compared to that was obtained with the proposed single element. The proposed antenna array is suitable for radar and microwave imaging applications where a directional UWB antenna is required.

References

[1] E. J. Thomas, "First Report And Order, Revision Of Part 15 Of The Commission's Rules Regarding Ultra-Wideband Transmission Systems Fcc, fcc02-48," May 2002. [Online]. Available: http:/ / www.fcc.gov/ Bureaus/ EngineeringTechnologies=Orders=2002=fcc02048:pdf

[2] M. E. Bialkowski, A. M. Abbosh, Y. Wang, D. Ireland, A. A. Bakar, and B. J. Mohammed, "Microwave Imaging Systems Employing Cylindrical, Hemispherical And Planar Arrays Of Ultrawideband Antennas," in *Microwave Conference Proceedings (APMC)*, 2011 Asia-Pacific, Dec 2011, pp. 191–194.

[3] L. Lewis, M. Fassett, and J. Hunt, "A Broadband Stripline Array Element," in *Antennas and Propagation Society International Symposium*, 1974, vol. 12, Jun 1974, pp. 335–337.

[4] J. Bourqui, M. A. Campbell, J. Sill, M. Shenouda, and E. C. Fear, "Antenna Performance For Ultra-Wideband Microwave Imaging," in *Radio and Wireless Symposium, 2009. RWS '09. IEEE*, Jan 2009, pp. 522–525.

[5] J. D. S. Langley, P. S. Hall, and P. Newham, "Novel Ultrawide-Bandwidth Vivaldi Antenna With Low Crosspolarisation," *Electronics Letters*, vol. 29, no. 23, pp. 2004–2005, Nov 1993.

[6] S. Maalik, "Antenna Design For UWB Radar Detection Application," Master dissertation, Dept. of Communication Engineering, Chalmers University of Technology, 2010.

[7] A. S. Atiah and N. J. Bowring, "Design Of flat Gain Uwb Tapered Slot Antenna For On-Body Concealed Weapons Detections," *PIERS Online*, vol. 7, no. 5, pp. 491–495, 2011.

[8] Y. Yang, Y. Wang, and A. E. Fathy, "Design Of Compact Vivaldi Antenna Arrays For Uwb See Through Wall Applications," *Progress In Electromagnetics Research*, vol. 82, pp. 401–418, 2008.

[9] A. Lazaro, R. Villarino, and D. Girbau, "Design Of Tapered Slot Vivaldi Antenna For Uwb Breast Cancer Detection," *Microwave and Optical Technology Letters*, vol. 53, no. 3, pp. 639–643, 2011. [Online]. Available: http:/ / dx.doi.org/ 10.1002/ mop.25770

[10] R. Natarajan, J. V. George, M. Kanagasabai, and A. K. Shrivastav, "A Compact Antipodal Vivaldi Antenna For UWB Applications," *IEEE Antennas and Wireless Propagation Letters*, vol. 14, pp. 1557–1560, 2015.

[11] L. Yang, H. Guo, X. Liu, H. Du, and G. Ji, "An Antipodal Vivaldi Antenna For Ultra-Wideband System," in *(ICUWB), 2010 IEEE International Conference on Ultra-Wideband*, vol. 1, Sept 2010, pp. 1–4.

[12] H. C. Ba, H. Shirai, and C. D. Ngoc, "Analysis And Design Of Antipodal Vivaldi Antenna For UWB Applications," in *(ICCE), 2014 IEEE Fifth International Conference on Communications and Electronics*, July 2014, pp. 391–394.

[13] Y. Wang, A. Bakar, and M. Bialkowski, "Reduced-Size Uwb Uniplanar Tapered Slot Antennas Without And With Corrugations," *Microwave and Optical Technology Letters*, vol. 53, no. 4, pp. 830–836, 2011. [Online]. Available: http:/ / dx.doi.org/ 10.1002/ mop.25878

[14] R. Singha and D. Vakula, "Corrugated Antipodal Vivaldi Antenna Using Spiral Shape Negative Index Metamaterial For Ultra-Wideband Application," in *(SPACES), 2015 International Conference on*

Signal Processing And Communication Engineering Systems, Jan 2015, pp. 179–183.

[15] A. M. D. Oliveira, M. B. Perotoni, S. T. Kofuji, and J. F. Justo, "A Palm Tree Antipodal Vivaldi Antenna With Exponential Slot Edge For Improved Radiation Pattern," *IEEE Antennas and Wireless Propagation Letters*, vol. 14, pp. 1334–1337, 2015.

[16] L. Chen, Z. Lei, R. Yang, J. Fan, and X. Shi, "A Broadband Artificial Material For Gain Enhancement Of Antipodal Tapered Slot Antenna," *IEEE Transactions on Antennas and Propagation*, vol. 63, no. 1, pp. 395–400, Jan 2015.

[17] I. T. Nassar and T. M. Weller, "A Novel Method For Improving Antipodal Vivaldi Antenna Performance," *IEEE Transactions on Antennas and Propagation*, vol. 63, no. 7, pp. 3321–3324, July 2015.

[18] K. Kota and L. Shafai, "Gain And Radiation Pattern Enhancement Of Balanced Antipodal Vivaldi Antenna," *Electronics Letters*, vol. 47, no. 5, pp. 303–304, March 2011.

[19] A. M. Abbosh and M. E. Bialkowski, "Design Of Ultrawideband Planar Monopole Antennas Of Circular And Elliptical Shape," *IEEE Transactions on Antennas and Propagation*, vol. 56, no. 1, pp. 17–23, Jan 2008.

[20] P. J. Gibson, "The Vivaldi Aerial," in *Microwave Conference*, 1979. 9th European, Sept 1979, pp. 101–105.

[21] S. Wang, X. D. Chen, and C. G. Parini, "Analysis Of Ultra Wideband Antipodal Vivaldi Antenna Design," in *Loughborough Antennas and Propagation Conference, LAPC*, April 2007, pp. 129–132.

[22] V. G. Veselago, "The Electrodynamics Of Substances With Simultaneously Negative Values Of ε And μ," *SOV PHYS USPEKHI*, vol. 10, no. 4, pp. 509–514, 1968.

[23] J. B. Pendry, A. J. Holden, W. J. Stewart, and I. Youngs, "Extremely Low Frequency Plasmons In Metallic Mesostructures," *Phys. Rev. Lett.*, vol. 76, pp. 4773–4776, Jun 1996. [Online]. Available: http:/ / link.aps.org/ doi/ 10.1103/ PhysRevLett.76.4773

[24] D. R. Smith, W. J. Padilla, D. C. Vier, S. C. Nemat-Nasser, and S. Schultz, "Composite Medium With Simultaneously Negative Permeability And Permittivity," *Phys. Rev. Lett.*, vol. 84, pp. 4184–4187, May 2000. [Online]. Available: http:/ / link.aps.org/ doi/ 10.1103/ PhysRevLett.84.4184

[25] M. M. Bilgic and K. Yegin, "Wideband Offset Slot-Coupled Patch Antenna Array For X/ Ku-Band Multimode Radars," *IEEE Antennas and Wireless Propagation Letters*, vol. 13, pp. 157–160, 2014.

[26] H. M. Bernety, R. Gholami, B. Zakeri, and M. Rostamian, "Linear Antenna Array Design For UWB Radar," in *IEEE Radar Conference (RADAR)*, April 2013, pp. 1–4.

[27] B. Kasi and C. K. Chakrabarty, "Ultra-Wideband Antenna Array Design For Target Detection," *Progress In Electromagnetics Research C*, vol. 25, pp. 67–79, 2012.